

Chlorine Adsorption on Silver (111) at Low Temperatures

Alex G. Shard*

School of Applied Science, The Robert Gordon University, St. Andrews Street,
Aberdeen, AB25 1HG, United Kingdom

Vinod R. Dhanak

IRC Surface Science, University of Liverpool, L69 3BX, United Kingdom

Received: November 9, 1999; In Final Form: January 18, 2000

Two previously unreported low-temperature structures of chlorine on silver(111) are discussed: the sharp Ag(111)–($\sqrt{3} \times \sqrt{3}$)R30°–Cl, which disorders above 195 K and a split spot pattern assigned as Ag(111)–(13×13)–Cl. The latter surface is also disordered at room temperature and gives a diffuse pattern reminiscent of a ($\sqrt{3} \times \sqrt{3}$) R30° pattern. These patterns are discussed with reference to previous work and compared to chlorine adsorption on other fcc transition metal (111) surfaces. SEXAFS analysis of the sharp Ag(111)–($\sqrt{3} \times \sqrt{3}$)R30°–Cl surface reveals a Cl–Ag bond length of 2.48 Å, which disagrees with a previous SEXAFS bond length determination for chlorine on Ag(111), but is in accordance with trends in metal–chlorine bond lengths for other fcc metal (111) ($\sqrt{3} \times \sqrt{3}$) R30° surfaces.

Introduction

Chlorine adsorption to the (111) face of silver has been the subject of a number of investigations, yet the literature displays no clear consensus regarding the chemistry and structural properties of this adsorbate/surface system.^{1–7} Rovida and Pratesi reported the appearance of a diffuse ($\sqrt{3} \times \sqrt{3}$) R30° structure at low coverages followed by a (3×3) saturation structure using dichloroethane as the source of chlorine.¹ Goddard and Lambert used Cl₂ gas as a source of chlorine and confirmed that a diffuse ($\sqrt{3} \times \sqrt{3}$) R30° was evident at low chlorine coverages (they assumed $\theta = 0.33$) and at higher coverages ($\theta = 0.49$) a (10×10) LEED pattern became evident at saturation.² This latter pattern was similar to a (3×3) in appearance and thought to be the same as that observed by Rovida and Pratesi. Both structures were interpreted as hexagonal overlayers of chlorine on an unreconstructed silver surface. A suggested reason for the poor definition of the ($\sqrt{3} \times \sqrt{3}$) R30° pattern was disorder of the chlorine layer (presumably due to thermal motion of chlorine atoms rather than small domain size). A later STM study³ gave a similar chlorine overlayer model for the saturated surface, but described the registry of the overlayer as (17×17). Other workers attribute the saturation pattern to an epitaxial AgCl(111) layer.⁴

Bowker and Waugh reported that adsorption of chlorine at 240 K resulted in an increased uptake of chlorine on the Ag(111) face compared to room temperature and postulated a layer growth mechanism at this temperature. At room temperature, chlorine was thought to dissolve in the bulk metal and was therefore not visible to Auger analysis. The chlorine coverage of the diffuse ($\sqrt{3} \times \sqrt{3}$) R30° structure was estimated to be within the range $0.67 < \theta < 1$.⁵

A structure for the diffuse ($\sqrt{3} \times \sqrt{3}$) R30° was proposed by Lamble et al. following a surface extended X-ray absorption fine structure (SEXAFS) investigation.⁶ This model consists of

a poorly ordered “vacancy honeycomb” or graphitic structure. Note that in this model the poor definition of the diffuse ($\sqrt{3} \times \sqrt{3}$) R30° structure is due to static disorder, with a small domain size causing broadness in the diffraction spots. Chlorine coverage for this structure is stated to be $\theta = 0.67$ and SEXAFS measurements were acquired at both room temperature and 100 K and at both $\theta = 0.67$ and $\theta = 0.33$. In all cases, the chlorine–silver bond length was determined to be 2.70 ± 0.01 Å, and within the honeycomb structure chlorine–chlorine separations are approximately 2.89 Å. These results are somewhat surprising when compared to similar metal–chlorine systems.⁷

Table 1 summarizes the adsorption behavior of chlorine onto the (111) face of 3d and 4d fcc metals including the results obtained for silver in this work. It is generally observed that at low chlorine coverages a sharp ($\sqrt{3} \times \sqrt{3}$) R30° LEED pattern emerges and this almost certainly correlates with $\theta = 0.33$. The structural determinations that have been performed on these surfaces suggest that the metal–chlorine bond length is between 2.3 and 2.4 Å. For silver, the Ag–Cl bond is estimated to be close to 2.51 Å using the method of Brown and Altematt.⁸ At higher coverages for the metals in Table 1 a number of other LEED patterns emerge, some of which require an annealing step. These patterns are mainly interpreted as coincident hexagonal chlorine overlayers, although some are undoubtedly due to metal–chlorine reconstructed surfaces or epitaxial growth of the metal halide.

The most notable difference between silver and these metals is that it does not display a sharp ($\sqrt{3} \times \sqrt{3}$) R30° structure at room temperature and $\theta = 0.33$. A somewhat closer inspection of the behavior of these structures indicates that it is fortunate that any of the ($\sqrt{3} \times \sqrt{3}$) R30° structures are observed at room temperature. The reported order–disorder temperatures of such surfaces are only slightly above room temperature and it is quite feasible that such a structure appears on the Ag(111) surface below room temperature. Heating the sharp ($\sqrt{3} \times \sqrt{3}$) R30° systems in Table 1 above the order/disorder transition results in a complete loss of fractional order spots,^{2,13,15} this would

* Corresponding author. E-mail: a.shard@rgu.ac.uk.

TABLE 1: Summary of Chlorine Induced Surface Structures on (111) Surfaces of 3d and 4d fcc Metals

metal	nickel	copper	rhodium	palladium	silver (this work)
M–Cl bond length ($\sqrt{3} \times \sqrt{3}$) R30° (Å)	2.33 ⁹	2.39 ¹¹	2.38 ¹²	2.39 ¹⁴	2.48
Cl adsorption site ($\sqrt{3} \times \sqrt{3}$) R30°	Hollow (fcc) ⁹	Hollow (fcc) ¹¹	probably hollow ¹²	unknown	unknown
order/disorder transition temp. ($\sqrt{3} \times \sqrt{3}$) R30°	unreported	350 K ²	380 K ¹³	350 K ¹⁵	195 K
structures interpreted as chlorine overlayers	$\begin{pmatrix} 2 & 1 \\ 4 & 7 \end{pmatrix}^{10}$	(12 $\sqrt{3} \times 12\sqrt{3}$) R30°, (4 $\sqrt{7} \times 4\sqrt{7}$) R19.2°, (6 $\sqrt{3} \times 6\sqrt{3}$) R30° ²	(4 × 4) ¹³	(4 × 4) ¹⁴	(13 × 13) (10 × 10) ²
structures interpreted as reconstructed metal chloride layers.			(4 × 4) ¹³	(4 × 4) “complex” ¹⁴	(10 × 10) ⁴

imply that the diffuse ($\sqrt{3} \times \sqrt{3}$) R30° observed on Ag(111) is not a disordered analogue of the sharp ($\sqrt{3} \times \sqrt{3}$) R30° structures observed on the earlier metals as suggested by Goddard and Lambert.²

The metal–chlorine bond length determined by SEXAFS is remarkably different for silver⁶ at $\theta = 0.33$ in comparison to other metals (see Table 1). The chlorine–chlorine nearest neighbor distance at $\theta = 0.67$ is reported to be approximately 2.89 Å,⁶ which is much less than double the van der Waals radius of chlorine (3.60 Å)⁷ and indicates significant Cl–Cl bonding interactions. No chlorine overlayer model for the metals given in Table 1 has interchlorine distances of less than 3.60 Å and thus chlorine on silver appears to display unique behavior that requires some explanation.

The motivation behind this work was to confirm the Cl–Ag bond length determined previously⁶ as it was not in accord with the Cl–Pd and Cl–Rh bond lengths we had found using SEXAFS.^{11,13} In the previous work on Ag(111), the X-ray absorption response was monitored by measuring the total electron yield (or drain current) of the sample as the photon energy was scanned through the Cl K-edge.⁶ This led to a step edge of approximately 2% of the background (EXAFS oscillations are generally less than 10% of the size of the step edge and so it can be seen that in the previous work drain current measurements were vastly dominated by background signal). In this study, we examine the adsorption of chlorine on silver at low temperatures and measure Cl K edge SEXAFS using X-ray fluorescence and Auger yield.

Experimental Section

Experiments were performed on beamline 4.2 (BL 4.2) of the Daresbury SRS. BL 4.2 has a standard UHV end chamber equipped with rear view LEED optics (Omicron) and a CLAM2 hemispherical analyzer (Vacuum Generators). The base pressure of the chamber was less than 3×10^{-10} mbar. The Ag(111) crystal was mounted onto an Omniax manipulator (VG) equipped with electron beam heating and liquid nitrogen cooling and cleaned by repeated cycles of argon ion bombardment and annealing until electron energy distribution curve (EDC) showed no trace of contamination and the LEED exhibited a sharp (1 × 1) pattern.

Chlorine was produced from an in situ solid-state electrochemical cell.¹⁶ Chlorine dosing was performed with the crystal facing the LEED optics and dosing was stopped when the required structures were observed. Experiments were carried out at room temperature (300 K) and with liquid nitrogen cooling (178 K). EDCs were taken with a photon energy of $h\nu = 2990$ eV, which is above the chlorine K-edge and the only elements observed on the crystal face throughout the experiments were chlorine and silver.

Chlorine K-edge (2833 eV) X-ray absorption spectra were recorded by monitoring both the Cl K fluorescence yield ($h\nu = 2620$ eV) with a gas proportional counter and the Cl LVV Auger yield (183 eV kinetic energy) with the hemispherical analyzer. Spectra were recorded with the surface normal at an angle of 30° to the incoming X-rays. The range of data acquired using Auger yield was limited by the coincidence of the Cl 1s and Cl LVV kinetic energies at $h\nu = 3000$ eV, but the fluorescence yield data could be used to monitor response up to the Ag L_{III} edge (3351 eV). Following background subtraction and normalization, the data were analyzed with the Excurv92 package using phase shifts calculated within the program.¹⁷

Results

Exposure of clean Ag(111) to chlorine at 178 K resulted in a series of LEED patterns which were observed reproducibly; see Figure 1. As the dosing time increased, diffuse rings first appeared around the integral order spots which eventually resolved into the first ordered structure. This was a sharp ($\sqrt{3} \times \sqrt{3}$) R30° pattern which appeared over a relatively limited time, first sharpening and then fading and broadening. The broadened $\sqrt{3}$ spots formed “V” shapes which in turn sharpened into three bright spots, with fainter fractional order spots also observable. The spot that is between and equidistant from the (1,0) and (0,1) spots is at (5/13, 5/13). Prolonged dosing resulted in the formation of a pattern identical to that observed by Goddard and Lambert and described by them as a (10 × 10).² Adsorption of chlorine at room temperature (300 K) on the same surface produced LEED patterns identical to those given in the literature.²

Heating the ($\sqrt{3} \times \sqrt{3}$) R30° surface to above 195 K resulted in the fractional order spots becoming abruptly diffuse and then completely lost at above 225 K, they reappeared on cooling to below 195 K. This order–disorder transition appeared to be very sharp and occurred over a small temperature range (approximately 2 K). The “three spot” pattern did not completely disappear after warming to room temperature; instead, the spots became diffuse and merged to give a pattern similar to the “diffuse” ($\sqrt{3} \times \sqrt{3}$) R30° seen during room-temperature adsorption of chlorine. Figure 1e shows this diffuse pattern at 250 K, at room temperature it was still observable but somewhat more diffuse and fainter.

By comparison of the Cl 1s peak areas from different surfaces the chlorine coverages were estimated. It was assumed that the sharp ($\sqrt{3} \times \sqrt{3}$) R30° corresponded to $\theta = 0.33$, which appears reasonable on the basis of chlorine adsorption on other fcc d-metals.^{2,9–14} The EDC intensities then indicate that the three-spot pattern corresponds to $\theta = 0.37 \pm 0.02$ and the pattern reported as (10 × 10) corresponds to $\theta = 0.45 \pm 0.02$. This latter chlorine coverage may not be definitive, as chlorine

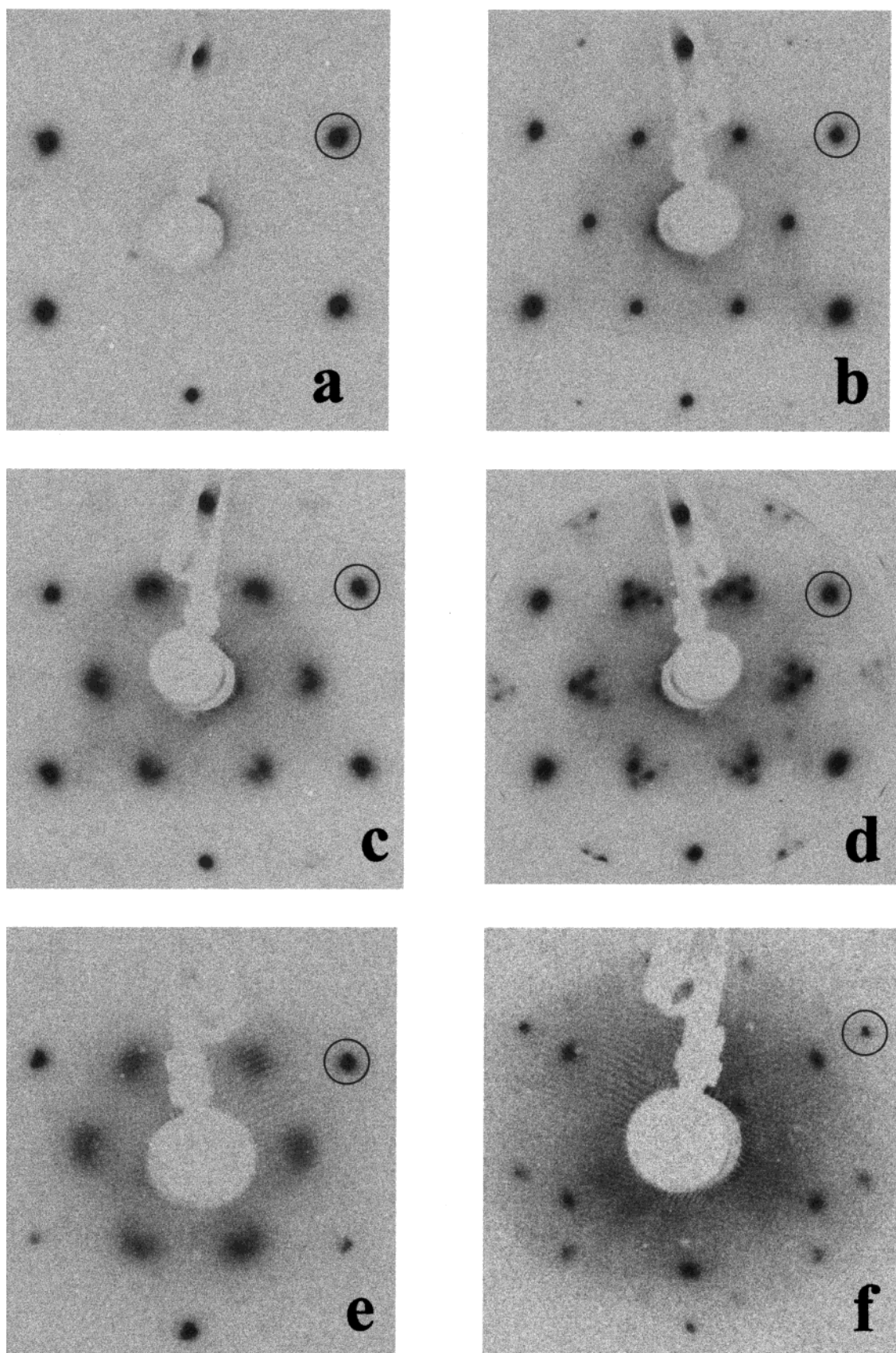


Figure 1. LEED patterns at 178 K of (a) clean Ag (1×1), (b) sharp Ag(111)-($\sqrt{3} \times \sqrt{3}$)R30°-Cl, (c) “V” shapes, (d) “split spot” Ag(111)-(13×13)-Cl, (e) same as (d) but at 250 K and (f) Ag(111)-(10×10)-Cl. All LEED patterns taken with $E_p = 50$ V except (e) $E_p = 59$ V and (f) $E_p = 80$ V. The (0,1) spot is circled in all figures.

adsorption at reduced temperature does not necessarily reach a limiting value for the total doses used in these experiments.⁵ At room temperature, a loss of chlorine was observed from the

$\theta = 0.33$ surface and the chlorine concentration was found to halve in approximately 2 h without dependence on X-ray exposure; no loss of chlorine was observed at 178 K.

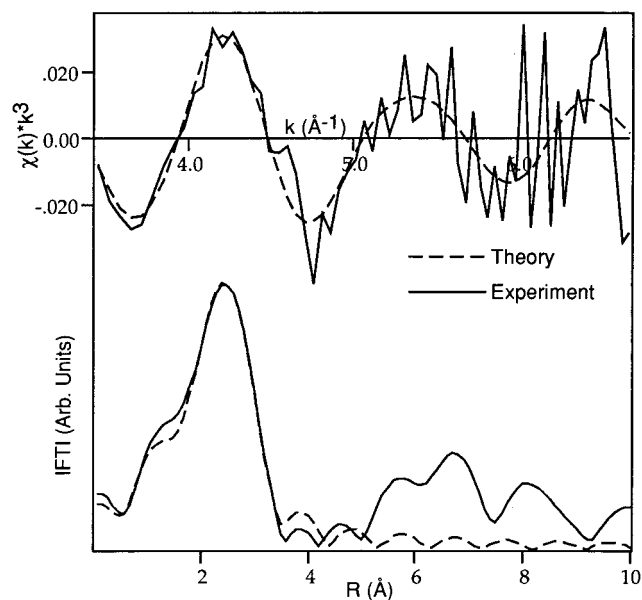


Figure 2. Cl K-edge EXAFS oscillations from the sharp Ag(111)–($\sqrt{3} \times \sqrt{3}$) R30°–Cl at 178 K following background subtraction, normalization to the edge step, and conversion into k -space (top) and the associated Fourier transform (bottom). Dashed line shows the best fit with a single shell of Ag atoms at a distance of 2.48 Å from the chlorine emitter.

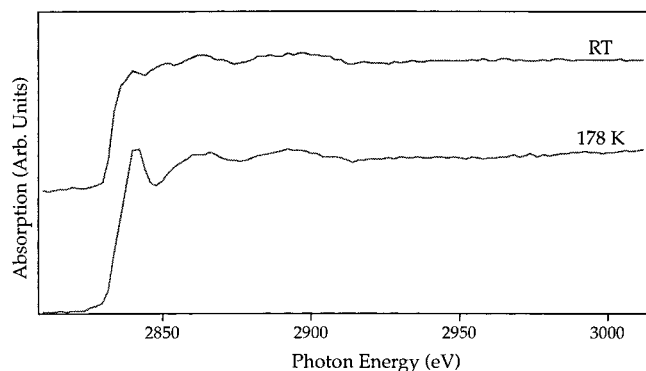


Figure 3. X-ray absorption spectra of the $\theta = 0.33$ surface at 178 K (bottom) and 300 K (top) demonstrating the disappearance of the sharp NEXAFS peak above the disordering temperature.

Cl K edge SEXAFS were taken from the sharp ($\sqrt{3} \times \sqrt{3}$) R30° surface at 178 K. Results from monitoring the Cl LVV Auger are shown in Figure 2. Analyses of data taken from Auger emission and X-ray fluorescence gave identical results, with the Auger data having a better signal/noise ratio. In both cases, the edge step was approximately 100% of the background signal, which is far greater than the total electron yield method.⁶ The EXAFS oscillations were found to damp rapidly and there was no indication of reliable or reproducible structure in the $\chi(k)$ functions for $k > 6$. This corresponded to a photon energy of less than 180 eV above the Cl K edge, and therefore the Cl 1s peak did not interfere with the Auger data within its usable range. The range and quality of data precluded a fit that included more than one shell of atoms and the best fit was found with a shell of silver atoms 2.48 ± 0.04 Å from the chlorine emitter.

Data taken from the sharp ($\sqrt{3} \times \sqrt{3}$) R30° surface at room temperature (i.e., above the disorder transition) did not demonstrate any significant difference in terms of SEXAFS oscillations; however, the near edge region of the absorption curve was markedly different and is shown in Figure 3. At 178 K there is a clear NEXAFS peak close to the adsorption edge, which has either been lost or been considerably broadened at

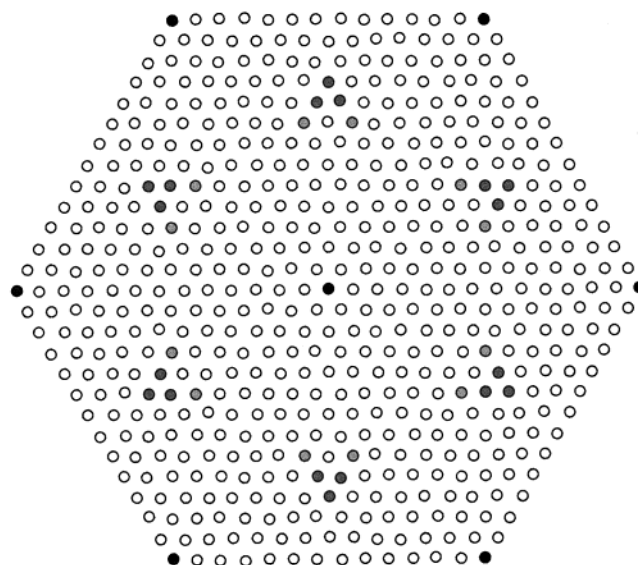


Figure 4. (13×13) pattern showing fractional order spots observed experimentally and shaded according to intensity in relation to integral order spots (black). Open circles indicate absences.

room temperature. There is no difference in chlorine coverage between these two spectra, and the loss of the NEXAFS peak is most likely related to the change of an ordered structure into a disordered one.

Discussion

The adsorption of chlorine onto Ag(111) at 178 K has revealed behavior that appears to be rather similar in its initial stages to adsorption of chlorine on Ni(111)¹⁰ and Cu(111)² at room temperature. In the case of these 3d metals, the first ordered superstructure is ($\sqrt{3} \times \sqrt{3}$) R30° followed by a split spot pattern similar to that shown in Figure 1. In both cases, these structures were interpreted as chlorine overlayers on an unreconstructed metal surface, in the case of copper the pattern was described as ($6\sqrt{3} \times 6\sqrt{3}$) R30°, and for nickel the matrix notation ($\frac{4}{2} \frac{1}{7}$) was used. On silver the observed spots appear to be best described as a (13×13) pattern; see Figure 4. The most intense spots are the (5/13, 4/13), (4/13, 5/13), and (5/13, 5/13), and providing a chlorine overlayer model is assumed, it would seem likely that one or all of these are related in reciprocal space to interchlorine separations in real space. This would imply interchlorine separations of either 4.35 or 4.81 Å. If it is assumed that the chlorine atoms form a hexagonal mesh on the surface, then the first interchlorine distance corresponds to $\theta = 0.44$ and the latter $\theta = 0.36$. An interchlorine separation of 4.81 Å in a hexagonal array is in good agreement with the chlorine coverage observed experimentally and implies that the (5/13, 4/13) and (4/13, 5/13) LEED spots relate to interchlorine directions and distances. If the assumptions made here are valid, then a structure such as that shown in Figure 5 can be proposed and the surface contains two domains which are related by a reflection and correspond to a rotation of the hexagonal mesh in either a clockwise or anticlockwise direction. A comparison to the proposed model for the ($\sqrt{3} \times \sqrt{3}$) R30° (also shown in Figure 5) surface demonstrates that the two surfaces are similar, with the (13×13) being related to the ($\sqrt{3} \times \sqrt{3}$) R30° following a uniform contraction of 4% and rotation by 3.7° of the chlorine overlayer. The close structural relationship of the ($\sqrt{3} \times \sqrt{3}$) R30° and (13×13) would imply that a number of intermediate structures could be formed and it is possibly these that give rise to the “V” shapes in the intermediate LEED

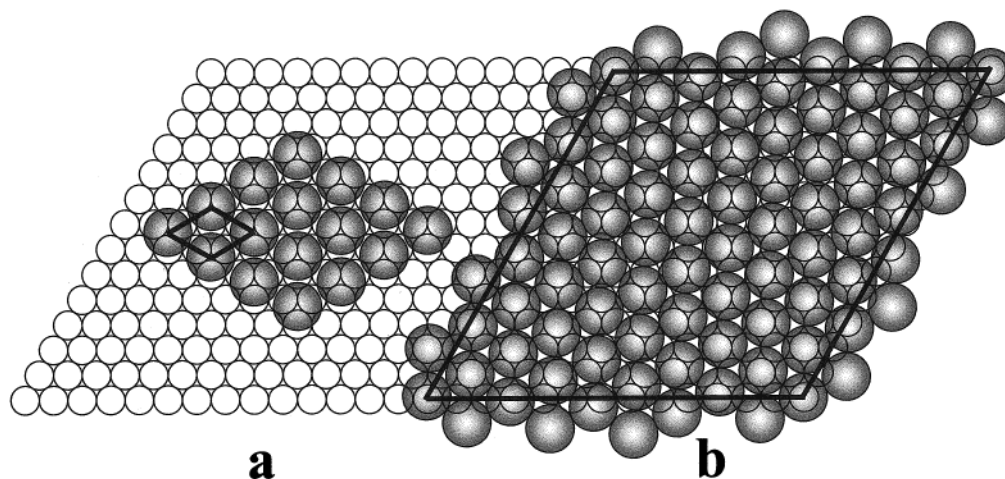


Figure 5. Overlayer models for the (a) $(\sqrt{3} \times \sqrt{3})$ R30° and (b) (13×13) surfaces. Silver atoms are shown as small, unfilled circles and chlorine atoms as the larger, shaded circles.

patterns (see Figure 1c). This structure is quite different from the graphitic structure proposed by Lamble et al.,⁶ but is in accordance with structures proposed for other fcc metal (111)–chlorine systems and maintains an interchlorine separation of greater than double the chlorine van der Waals radius.

It seems likely, on the basis of our observations that the diffuse $(\sqrt{3} \times \sqrt{3})$ R30° observed at room temperature is, in fact, a diffuse (13×13) . This would rule out the “static disorder” graphitic model of Lamble et al.⁶ If the room-temperature structure is a diffuse (13×13) , then our reported coverage of $\theta = 0.37$ is somewhat different from previous investigations, which are outlined in the Introduction. An explanation of this discrepancy is that previous workers had not identified the sharp $(\sqrt{3} \times \sqrt{3})$ R30° structure and were thus assigning coverages without a reliable reference point. If we correct previous reports of chlorine coverage for the structure reported as (10×10) based on the assumption that the diffuse (13×13) coverage is $\theta = 0.37$, we find that Goddard and Lambert² give $\theta = 0.54$ and Bowker and Waugh⁵ $\theta = 0.49$. These compare reasonably well to our determination of $\theta = 0.45$ especially if it is considered that our value was recorded after the (10×10) was initially observed and Bowker and Waugh⁵ report that chlorine adsorption continues after this pattern is first seen.

The loss of chlorine from the $\theta = 0.33$ surface occurs slowly at room temperature; it is likely that chlorine atoms become dissolved in the subsurface or bulk of the silver crystal, as postulated previously.⁵

SEXAFS of the sharp $(\sqrt{3} \times \sqrt{3})$ R30° gave a Cl–Ag bond length of 2.48 Å, in good agreement with the calculated value of 2.51 Å. It is remarkably different from the previous report of 2.70 Å.⁶ This discrepancy deserves some comment. First, it should be noted that the surfaces examined were, in fact, somewhat different in these two studies. Lamble et al.⁶ report bond lengths for $\theta = 0.33$ and 0.67 (which can be corrected to $\theta = 0.19$ and 0.37) at temperatures of 300 and 100 K. With the corrected coverages and temperatures the sharp $(\sqrt{3} \times \sqrt{3})$ R30° is not formed; however, the (13×13) should have been observed but was not reported. This is not overly surprising if the exact coverage for the (13×13) was not obtained, the blurred “V” shapes can be mistaken for a diffuse $(\sqrt{3} \times \sqrt{3})$ R30° pattern.

The major difference between the previous SEXAFS work and ours is that a different mode of detection was used. Auger electron and fluorescent X-ray detection are substantially more

sensitive than total electron yield measurements, yet it was our observation that the intensity of Cl K-edge SEXAFS oscillations diminishes rapidly as the photoelectron kinetic energy increases. This is to be expected if the chlorine atoms have significant vibrational motion around their average positions. The low disordering temperatures of these surfaces support the idea of a large population of vibrationally excited states in the chlorine overlayer. Our experiences with similar systems also indicate that reliable EXAFS structure is rarely found for $k > 6\text{--}7 \text{ \AA}^{-1}$, whereas Lamble et al.⁶ claim to have structure to at least $k = 9 \text{ \AA}^{-1}$ even at room temperature, using a less sensitive detection method than was used in this work. It is our opinion that much of the structure observed in the previous work was introduced from variations in background rather than from the chlorine overlayer. These effects can be reproducible if they arise, for example, from contaminants on beam line optics or irregularities in the monochromator drive, and become more pronounced if the signal-to-background ratio is small.

The Cl K edge NEXAFS peak observed for the sharp $(\sqrt{3} \times \sqrt{3})$ R30° structure at 178 K is similar to that observed on Pd(111)– $(\sqrt{3} \times \sqrt{3})$ R30°–Cl¹³ in which it was assigned to a promotion of the K electron to a partially filled Cl p_z band. At room temperature, the NEXAFS transition is no longer observed and this may be taken as an indication of disorder in the chlorine overlayer.

The disorder temperature of the sharp $(\sqrt{3} \times \sqrt{3})$ R30° structure (195 K) is much lower than the other 4d and 3d fcc metals given in Table 1. It is thought⁷ that one of the major factors lending stability to these structures is repulsive interactions between adjacent chlorine atoms. Therefore, if chlorine–metal interactions are ignored it would be expected that order–disorder transition temperatures would increase as the chlorine–chlorine separation decreases. If all these surfaces have chlorine coverage of $\theta = 0.33$ the interchlorine distances decrease in the order Ag(111) > Pd(111) > Rh(111) > Cu(111) > Ni(111). The disordering temperatures of the Pd and Rh systems are higher than would be expected on the basis of the Cu and Ag systems and it must be concluded that chlorine–metal interactions are rather important in stabilizing some, if not all of these systems. If the argument is applied only to the group 11 metals (Cu, Ag, Au) the $(\sqrt{3} \times \sqrt{3})$ R30° disorder temperature would be expected to be lowest for silver, with gold having a slightly higher disordering temperature as a consequence of its slightly smaller unit cell dimensions. A sharp $(\sqrt{3} \times \sqrt{3})$ R30° structure has been observed for chlorine on Au(111)¹⁸ by Kastanas and

Koel which reversibly disorders at 230 K; however, the authors assign this LEED pattern to a coverage of $\theta = 1.33$ with their model having interchlorine separations of 2.48 Å, a great deal less than double the van der Waals radius and implying chlorine–chlorine bonding interactions. Even more remarkably, this pattern appears at only half of the saturation coverage for chlorine on Au(111). The authors base their coverage calculations on estimated AES sensitivity factors, which may not be totally reliable. It would seem more likely that the Au(111)–($\sqrt{3} \times \sqrt{3}$) R30°–Cl surface correlates with $\theta = 0.33$ and the disorder transition temperature is slightly higher than Ag(111)–($\sqrt{3} \times \sqrt{3}$) R30°–Cl as expected.

Conclusions

Two new structures of chlorine on Ag(111) are reported. These are the sharp ($\sqrt{3} \times \sqrt{3}$) R30° and the (13×13), both of which are only observed at low temperatures. The chlorine–silver bond length has been measured by SEXAFS for the sharp ($\sqrt{3} \times \sqrt{3}$) R30° surface and found to be 2.48 Å, this is in disagreement with earlier SEXAFS work on similar surfaces, but agrees well with trends observed for chlorine adsorption on other fcc transition metal (111) surfaces. We postulate that the room-temperature surface identified as a diffuse ($\sqrt{3} \times \sqrt{3}$) R30° is in fact a diffuse (13×13). Assuming that the sharp ($\sqrt{3} \times \sqrt{3}$) R30° surface corresponds to $\theta = 0.33$, chlorine coverages from previous investigations are reinterpreted and found to be in reasonable agreement with this work. The low temperature of the order–disorder transition of the sharp Ag(111)–($\sqrt{3} \times \sqrt{3}$) R30°–Cl surface can be explained in terms of reduced interchlorine repulsion due to greater interchlorine separations in comparison to similar surfaces on other 3d and 4d fcc transition metals.

Acknowledgment. We thank the Liverpool IRC in surface science for the provision of beamtime and also G. Miller and G. Bray for their advice and technical assistance. We also thank D. Norman for interesting discussions.

References and Notes

- (1) Rovida, G.; Pratesi, F. *Surf. Sci.* **1975**, *51*, 270.
- (2) Goddard, P. J.; Lambert, R. M. *Surf. Sci.* **1977**, *67*, 180.
- (3) Andryushechkin, B. V.; Eltsov, K. N.; Shevlyuga, V. M.; Yurov, V. Y. *Surf. Sci.* **1998**, *407*, L633.
- (4) Wu, K.; Wang, D.; Deng, J.; Wei, X.; Cao, Y.; Zei, M.; Zhai, R.; Guo, X. *Surf. Sci.* **1992**, *264*, 249. Tu, Y. Y.; Blakely, J. M. *J. Vac. Sci. Technol.* **1978**, *15*, 563. Tu, Y. Y.; Blakely, J. M. *Surf. Sci.* **1979**, *85*, 276.
- (5) Bowker, M.; Waugh, K. C. *Surf. Sci.* **1983**, *134*, 639.
- (6) Lamble, G. M.; Brooks, R. S.; Ferrer, S.; King, D. A.; Norman, D. *Phys. Rev. B* **1986**, *34*, 4, 2975.
- (7) Jones, R. G. *Prog. Surf. Sci.* **1988**, *27*, 25.
- (8) Mitchell, K. A. R.; Schlatter, S. A.; Sodhi, R. N. S. *Can. J. Chem.* **1986**, *64*, 1435. Brown, I. D.; Altermatt, D. *Acta Crystallogr.* **1985**, *B41*, 244.
- (9) Wang, L. Q.; Hussain, Z.; Huang, Z. Q.; Schach von Wittenau, A. E.; Lindle, D. W.; Shirley, D. A. *Phys. Rev. B* **1991**, *44*, 24, 13711. Funabashi, M.; Yokoyama, T.; Takata, Y.; Ohta, T.; Kitajima, Y.; Kuroda, H. *Surf. Sci.* **1991**, *242*, 59.
- (10) Erley, W.; Wagner, K. *Surf. Sci.* **1977**, *66*, 371.
- (11) Woodruff, D. P.; Seymour, D. L.; McConville, C. F.; Riley, C. E.; Crapper, M. D.; Prince, N. P.; Jones, R. G. *Phys. Rev. Lett.* **1987**, *58* (14), 1460. Crapper, M. D.; Riley, C. E.; Sweeney, P. J. J.; McConville, C. F.; Woodruff, D. P.; Jones, R. G. *Surf. Sci.* **1987**, *182*, 213.
- (12) Shard, A. G.; Dhanak, V. R.; Santoni, A. *Surf. Sci.* **1999**, *429*, 279.
- (13) Cox, M. P.; Lambert, R. M. *Surf. Sci.* **1981**, *107*, 547.
- (14) Shard, A. G.; Dhanak, V. R.; Santoni, A. *Surf. Sci.*, in press.
- (15) Shard, A. G.; Dhanak, V. R. Unpublished observations.
- (16) Spencer, N. D.; Goddard, P. J.; Davies, P. W.; Kitson, M.; Lambert, R. M. *J. Vac. Sci. Technol.* **1989**, *A7*, 1554.
- (17) Gurman, S. J. *Synchrotron. Radiat.* **1995**, *2*, 56.
- (18) Kastanas, G. N.; Koel, B. E. *Appl. Surf. Sci.* **1993**, *64*, 235.